

Scandium-Decorated MOF-5 as Potential Candidates for Room-Temperature Hydrogen Storage: A Solution for the Clustering Problem in MOFs

Mudit Dixit,[†] Tuhina Adit Maark,[‡] Kamalika Ghatak,[†] Rajiv Ahuja,^{‡,§} and Sourav Pal^{*,†}

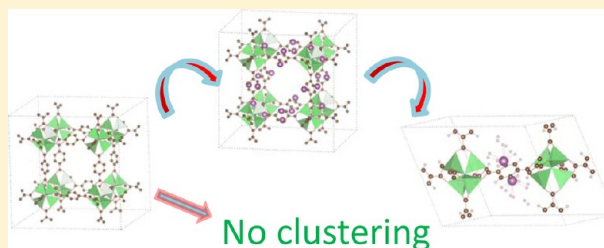
[†]Electronic Structure Theory Group, Physical and Material Chemistry Division, National Chemical Laboratory (CSIR), Pune-411 008, India

[‡]Condensed Matter Theory Group, Department of Physics and Astronomy, Box 516, Uppsala University, SE-751 20 Uppsala, Sweden

[§]Applied Materials Physics, Department of Materials Science and Engineering, Royal Institute of Technology (KTH), SE-100 44 Stockholm, Sweden

S Supporting Information

ABSTRACT: Transition-metal-based systems show promising binding energy for hydrogen storage but suffer from clustering problem. The effect of light transition metal ($M = \text{Sc}, \text{Ti}$) decoration, boron substitution on the hydrogen storage properties of MOF-5, and clustering problem of metals has been investigated using ab initio density functional theory. Our results of solid-state calculations reveal that whereas Ti clusters strongly Sc atoms do not suffer from this problem when decorating MOF-5. Boron substitution on metal-decorated MOF-5 enhances the interaction energy of both the metals with MOF-5. Sc-decorated MOF-5 shows a hydrogen storage capacity of 5.81 wt % with calculated binding energies of 20–40 kJ/mol, which ensures the room-temperature applicability of this hydrogen storage material.



Because of the high energy density, efficient burning within fuel cell technology, high abundance and environmentally clean nature, hydrogen has attracted vast research interest¹ as an alternative to our dependence upon fossil fuels. However, the need for a safe and competent (high gravimetric and volumetric density) storage system is the key challenge for practical commercialization of hydrogen-powered mobile or static applications. Technical targets established by the U.S. Department of Energy (DOE) require 5.5 wt % gravimetric and 40 g of H_2/L volumetric storage by the year 2015. Over the past decade, a number of research efforts have been made to find new storage materials to achieve the established storage targets.

Simple and complex metal hydrides are promising materials for hydrogen storage. Although these materials exhibit a high H_2 storage capacity, they suffer from large dehydrogenation activation barriers. In an interesting study, Kelkar et al.² have shown that doping different phases of MgH_2 with Al and Si can result in a lowering of its activation energy barriers associated with the direct desorption of H_2 from its (001) surface.

A variety of porous materials have been widely tested experimentally and theoretically,³ including covalent organic frameworks (COFs) and metal organic frameworks (MOFs). MOFs are crystalline hybrid organic/inorganic nanoporous materials, which can adsorb guest molecules and thus are potential candidates for H_2 storage.⁴ Because of the predominant contribution of van der Waals interactions between the physisorbed H_2 molecules and the host MOFs, the resulting H_2 adsorption enthalpies are typically in the range

of 2.2–5.2 kJ/mol.^{5–7} As a result, MOFs exhibit fast adsorption/desorption kinetics.

A study by Lochan and Head-Gordon⁸ depicts that the ideal H_2 binding energy range is 20–40 kJ/mol for storage under established target conditions (–20 to 50 °C and at 100 bar). H_2 binding energies in this range ensure reversibility and fast adsorption/desorption kinetics. A major challenge is thus to tune the H_2 binding energy as well as increase the H_2 adsorption of MOFs to render them useful for practical and mobile applications. For this, the introduction of interactions other than van der Waals is necessary in MOFs. A widely accepted strategy is the introduction of charged species in MOFs for achieving the desired H_2 binding energy.^{9,10}

Many theoretical studies have been focused upon the interaction of H_2 molecules with metal ions.^{10–15} Many research studies explored extensively the possibility of storing hydrogen via the Kubas interaction transition metal (TM)-decorated graphitic nanostructures^{16–24} (nanotubes, fullerenes, and graphene). In a well-known study of TM decoration, Yildirim et al.²⁰ illustrated that Ti-decorated nanotubes can adsorb up to 8 H_2 per Ti with a high binding energy of 0.43 eV/ H_2 with hydrogen uptake up to 8 wt %.

Decoration of alkali and alkaline earth metals has also been investigated theoretically on several systems, including carbon

Received: March 26, 2012

Revised: July 5, 2012

Published: July 26, 2012



Table 1. Structural Parameters of MOF-5, MOF-M₂, MOF:M₂:nH₂, MOF:2B:Sc₂, and MOF:2B:Sc₂:nH₂ Systems^a

system	C ₁ –C ₂	C ₂ –C ₃	C ₃ –C ₃	M–BZ _{COM}	M–H ₂	M–H ₂	M–H ₂	M–H ₂	H–H (average distance)
MOF-5	1.498	1.403	1.391						
MOFSc ₂	1.476	1.472	1.461	1.767					
MOF:Sc ₂ :2H ₂	1.471	1.477	1.467	1.760	2.12				0.81
MOF:Sc ₂ :4H ₂	1.466	1.469	1.465	1.790	2.11	2.11			0.81
MOF:Sc ₂ :6H ₂	1.466	1.469	1.460	1.819	2.18	2.15	2.21		0.79
MOF:Sc ₂ :8H ₂	1.460	1.469	1.448	1.834	2.22	2.29	2.24	2.29	0.77
MOF:Sc ₂ :10H ₂	1.459	1.469	1.446	1.830	2.25	2.26	2.23	2.82	0.77(0.75)
MOF:Ti ₂	1.485	1.479	1.463	1.631					
MOF:Ti ₂ :2H ₂	1.475	1.466	1.460	1.72	1.72				1.95
MOF:Ti ₂ :4H ₂	1.479	1.451	1.447	1.760	1.87	1.87			0.90
MOF:Ti ₂ :6H ₂	1.487	1.451	1.454	1.769	1.9	1.9	1.9		0.85
MOF:Ti ₂ :8H ₂	1.467	1.460	1.433	1.792	1.9	2.0	1.95	1.96	0.81
MOF:Ti ₂ :10H ₂	1.465	1.461	1.433	1.785	2.0	1.99	2.0	2.0(3.86)	0.80(0.75)
MOF:2B:Sc ₂	1.547	1.570	1.472	1.652					0.78
MOF:2B:Sc ₂ :2H ₂	1.548	1.577	1.478	1.668	2.22				0.78
MOF:2B:Sc ₂ :4H ₂	1.549	1.564	1.475	1.698	2.19	2.19			0.78
MOF:2B:Sc ₂ :6H ₂	1.552	1.558	1.465	1.747	2.17	2.17	2.22		0.78
MOF:2B:Sc ₂ :8H ₂	1.567	1.544	1.446	1.898	2.0	2.0	2.0	2.1	0.80
MOF:2B:Sc ₂ :10H ₂	1.556	1.552	1.450	1.819	2.12	2.11	2.16	2.17(3.83)	0.78

^aValues given in () correspond to fifth hydrogen per metal. M–BZ_{COM} is the distance of metal atom from benzene of MOF-5.

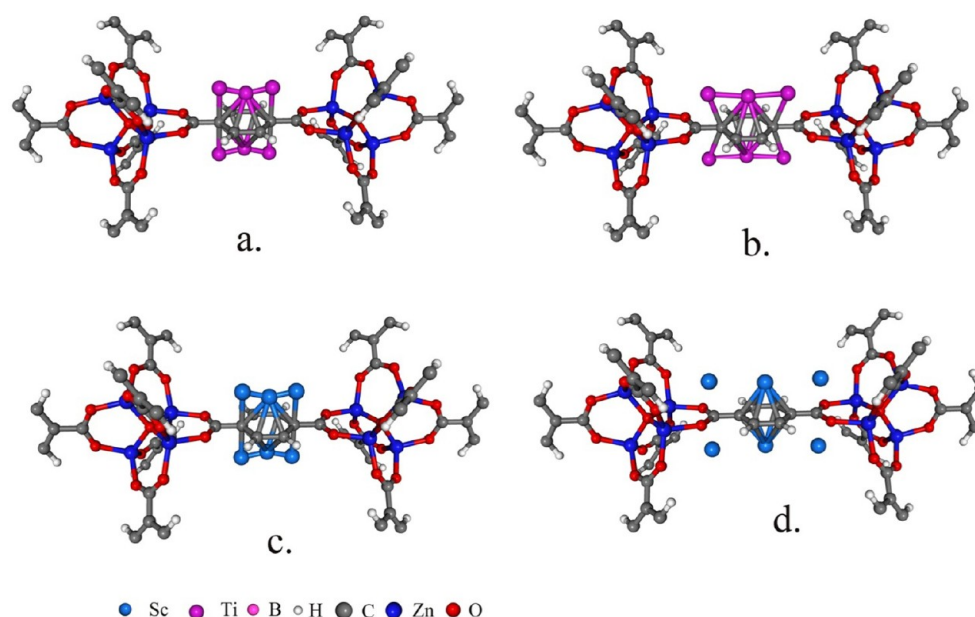


Figure 1. (a) Initial geometry of MDM where six Ti metals are decorated on MOF-5. (b) Relaxed geometry of MDM where six Ti metals are decorated on MOF-5. (c) Initial geometry of MDM where six Sc metals are decorated on MOF-5. (d) Relaxed geometry of MDM where six Sc metals are decorated on MOF-5.

nanotubes (CNTs), graphene, and fullerenes.^{25–40} The prime problem with TM-based materials is the tendency of metal atoms to cluster among each other.^{41,42} It has been shown⁴¹ that TM atoms cluster on the surface of C₆₀, which significantly reduces the storage capacity. To prevent the clustering of metal atoms, the doping of carbon nanostructures by boron has also been proposed.¹⁸

It is well known that methods based on DFT are unable to describe correctly dispersion and van der Waals interactions. Furthermore, ab initio methods such as MP2 and CCSD (T) are not practical for application to the full structure. However, in metal-decorated systems the electrostatic contributions are predominant. Thus, DFT methods provide reasonably accurate results for such systems. In a recent study,⁴³ we have shown

that the PBE-PAW plane-wave method gives reasonable H₂ binding energy for metal-decorated MOF-5 when compared with cc-pVTZ/MP2.

The objective of this study is three-fold: first, to identify potential hydrogen storage candidate with incorporation of Kubas interaction; second, to search for the best light TM atom that can increase the strength of H₂ adsorption, enhance the amount of H₂ storage in MOF-5, and does not suffer from the well-known clustering problem in MOFs; and third, to investigate whether boron substitution can avoid the clustering problem of TMs. Therefore, herein we investigate Sc- and Ti-decorated MOF-5 systems and their hydrogen binding energies (*E*_{binding}) and storage capacities using periodic DFT-based calculations employing the PBE functional. Furthermore, 1,4-

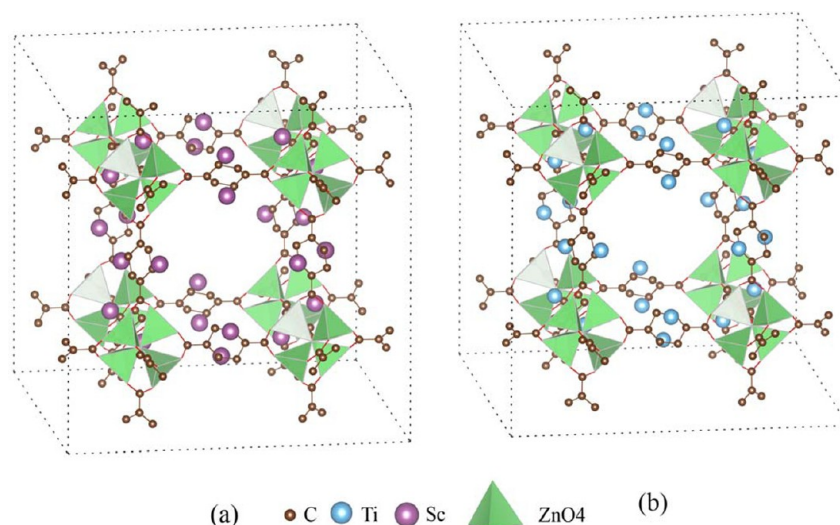


Figure 2. (a) Optimized geometry of full-MDM, where 24 Sc metal atoms are decorated on MOF-5. (b) Optimized geometry of full-MDM where 24 Ti metal atoms are decorated on MOF-5.

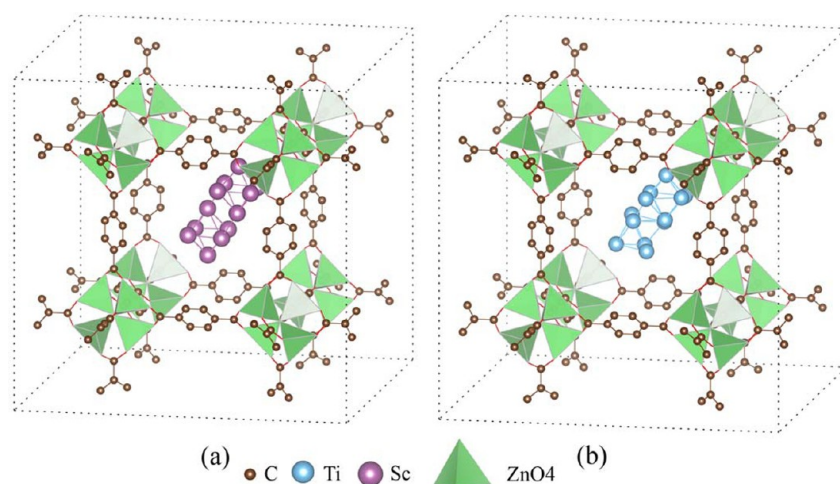


Figure 3. (a) Optimized geometry of full-MOF-5 where a cluster of 12 Sc metal atoms relaxed inside the pore. (b) Optimized geometry of full-MOF-5 where a cluster of 12 Ti metal atoms relaxed inside the pore.

boron-substituted metal-decorated MOF-5 are also investigated.

We first investigate individual interactions of the bare metal atoms with up to $n = 8$ H_2 molecules. The corresponding structures are displayed in Figures S1 and S2 of the Supporting Information, whereas the E_{binding} and charge on the metal atoms are presented in Table S1 of the Supporting Information. H_2 binding energies are found to be between -113.31 and -33.02 kJ/mol for $\text{Sc-}n\text{H}_2$ and between -95.59 and -41.12 kJ/mol for $\text{Ti-}n\text{H}_2$. These results confirm that both Sc and Ti have potential for hydrogen storage.

As a next step, we analyzed the corresponding metal-decorated MOF-5s (MDMs). The adsorption of metal atoms (Sc and Ti) on the MOF-5 was investigated by fully optimizing the structures with metal atoms initially placed close to the aromatic ring center of MOF-5. Both Sc and Ti show high interaction energy with MOF-5 of -281.32 and -244.04 kJ/mol, respectively.

The geometrical changes induced on MOF-5 as a result of metal decoration can be understood by comparing the C–C bond lengths of the aromatic ring listed in Table 1. It is clear

from the Table that both metal atoms induce a stretching of the aromatic ring with a shortening of $\text{C}_1\text{--C}_2$ and an increase in $\text{C}_2\text{--C}_3$ and $\text{C}_3\text{--C}_3$ distance, indicating that a charge transfer takes place from metal atoms to the MOF-5 framework. The $\text{C}_1\text{--C}_2$ bond contractions, in particular, become more predominant when more H_2 molecules are allowed to interact with the MDM.

Bader analysis⁴⁴ of the self-consistent charge density revealed that Sc and Ti atoms carry a charge of 1.12 and 1.1 e per metal, respectively (See Figure S4 of the Supporting Information). This implies that the electronic charge has been produced due to the large difference in the electronegativities of the metal atoms and MOF-5. This charge will be critically beneficial in raising the H_2 binding affinity.

It is well known that TMs prefer to cluster among each other; this clustering then reduces their binding energy as well as H_2 storage capacity. Therefore, we have studied the clustering of these TMs on MOF-5. As shown in Figure 1, initially three metal atoms were decorated on each side of benzene ring in MOF-5 (six metals atoms on primitive cell) at a close M–M distance of 1.51 Å from each other. On relaxation,

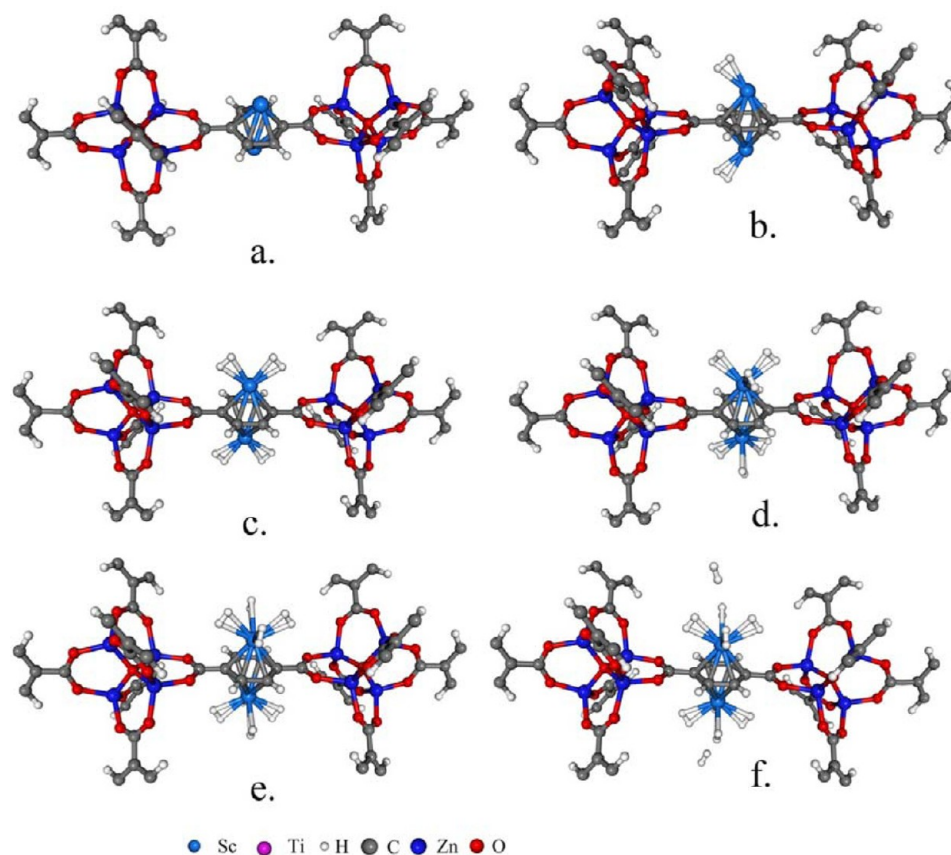


Figure 4. Relaxed structures of (a) MOF:Sc₂ and MOF:Sc₂:*n*H₂ (b) 2H₂, (c) 4H₂, (d) 6H₂, (e) 8H₂, and (f) 10H₂.

Sc atoms were found to be far apart (3.1 Å), whereas the Ti atoms were relatively close to each other at 2.10 Å. This confirms that Sc atoms do not cluster on MOF-5 but Ti atoms do. Further affirmation of this comes from the Bader charge analysis. Sc atoms in MOF-5:Sc₆ maintain their charge of 0.9 e, but the charge on Ti atoms in MOF-5:Ti₆ (0.45 e) is much reduced compared with MOF-5:Ti₂.

To confirm that Sc atoms do not cluster on MOF-5, we have optimized the full unit-cell of MOF-5, full metal-decorated MOF-5 (MOF:M₂₄) (Figure 2a,b), and M₁₂ cluster inside the MOF-5 (MOF:M₁₂) (Figure 3a,b). In full unit cell of MOF-5, there are 12 BDC facing toward inside, and thus we have taken M₁₂ cluster inside the MOF-5 pore. The difference in the formation energy of both atomic and clustered configuration indicates whether the metal clusters inside the MOF or remains in atomic nonclustered form. The formation energy per metal of clustered configuration is given as

$$E_f^c = \frac{1}{12} [E_T(\text{MOF: } M_{12}^c) - E_T(\text{MOF}) - 12E_T^a(M)] \quad (1)$$

whereas the formation energy per metal of atomic nonclustered configuration is given as

$$E_f^a = \frac{1}{24} [E_T(\text{MOF: } M_{24}^a) - E_T(\text{MOF}) - 24E_T^a(M)] \quad (2)$$

The difference in the formation energy of both atomic and clustered configuration is given as:

$$\Delta E_a^c = E_f^a - E_f^c \quad (3)$$

If ΔE_a^c is positive, then clustering is favored, and if ΔE_a^c is negative, then nonclustered atomic configuration is favored. $\Delta E_a^c(\text{Sc})$ is found to be −0.31 eV, whereas $\Delta E_a^c(\text{Ti})$ is found to be 1.29 eV. These results clearly prove that Ti clusters strongly inside MOF, whereas Sc does not cluster within MOF.

In a recent study,⁴⁵ it was shown that lithium-decorated MOF has been prepared via impregnating MOF with an ethanol solution of LiNO₃, followed by heat treatment in the vacuum. Similar strategy can be followed for synthesizing Sc-decorated MOF-5.

The molecular frequency calculations on Sc₂–BDC units suggested that Sc₂–BDC correspond to stable minima (Figures S5.a and S5.b of the Supporting Information) in both ethanol and water.

The above results open up a possibility to realize a TM (Sc)-decorated MOF-5 as a potential hydrogen storage candidate, which does not suffer from the clustering problem. Therefore, we also perform a comparative study of MOF-5:M₂ (where M = Sc and Ti) with regard to their interaction with increasing number of H₂. The fully optimized geometries of MOF-5:M₂:2*n*H₂ (where *n* = 1, 2, ..., 5) are displayed in Figure 4 and Figure S3 of the Supporting Information. The adsorption energies were calculated as

$$E_{\text{binding}} = \frac{1}{2n} \{E_T(\text{MOF: } M_2: 2nH_2) - E_T(\text{MOF: } M_2) - 2nE_T(H_2)\} \quad (4)$$

where $E_T(\text{MOF:M}_2:2nH_2)$, $E_T(\text{MOF:M}_2)$, and $E_T(H_2)$ are the total energies of MOF:M₂:2*n*H₂, MOF:M₂, and H₂ molecule, respectively. The E_{binding} are listed in Table 2. We found binding

Table 2. Binding Energies of MOF:M₂:*n*H₂ and MOF:2B:Sc₂:*n*H₂ Systems

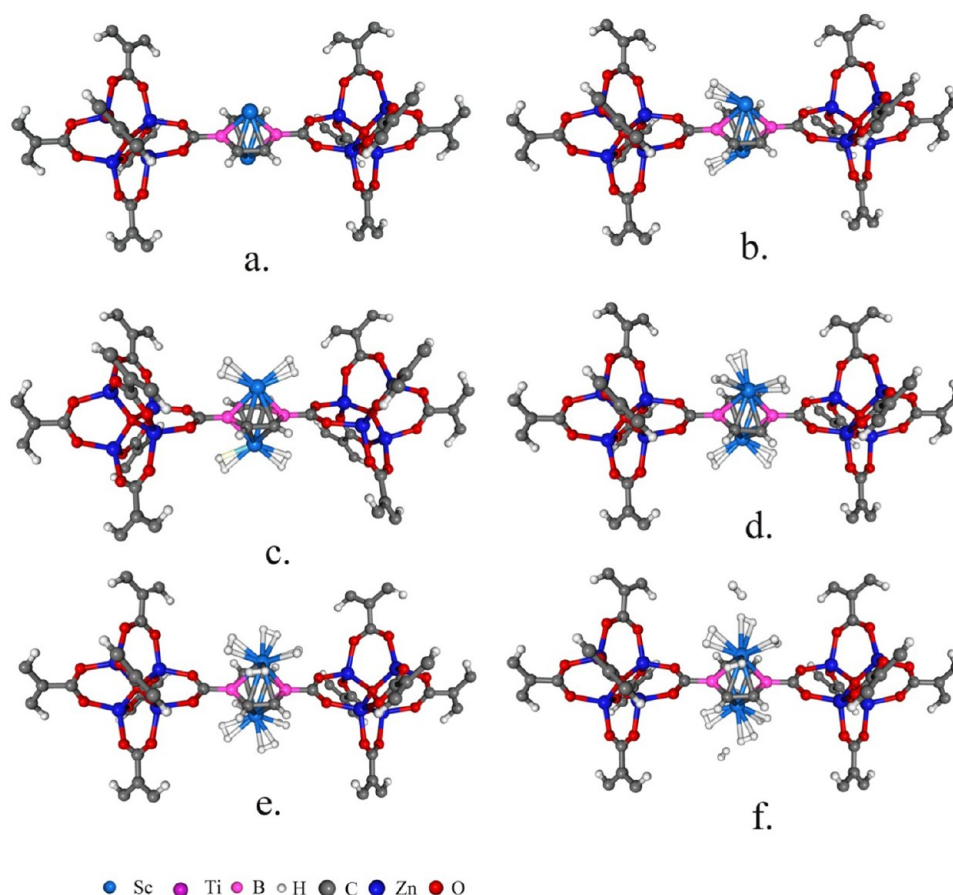
system	total binding energy(kJ/mol)	BE/H ₂
MOF:Sc ₂ :2H ₂	−40.55	−20.27
MOF:Sc ₂ :4H ₂	−129.82	−32.45
MOF:Sc ₂ :6H ₂	−178.02	−29.67
MOF:Sc ₂ :8H ₂	−194.28	−24.28
MOF:Sc ₂ :10H ₂	−209.29	−20.92
MOF:Ti ₂ :2H ₂	−196.13	−98.06
MOF:Ti ₂ :4H ₂	−298.00	−74.500
MOF:Ti ₂ :6H ₂	−401.04	−66.84
MOF:Ti ₂ :8H ₂	−398.37	−49.79
MOF:Ti ₂ :10H ₂	−393.57	−39.35
MOF:2B:Sc ₂ :2H ₂	−47.74	−23.87
MOF:2B:Sc ₂ :4H ₂	−111.85	27.96
MOF:2B:Sc ₂ :6H ₂	−153.88	−25.64
MOF:2B:Sc ₂ :8H ₂	−217.85	−27.23
MOF:2B:Sc ₂ :10H ₂	−199.80	−19.88

energies of 20.27 kJ/mol H₂ for *n* = 1, 32.45 kJ/mol H₂ for *n* = 2, 29.67 kJ/mol H₂ for *n* = 3, 32.29 kJ/mol H₂ for *n* = 4, and 19.46 kJ/mol H₂ for *n* = 5 for Sc-decorated MOF. The binding energies of Ti-decorated MOF-5 were found to be higher lying in range of −98.06 to −39.35 kJ/mol H₂ for *n* = 1–5. Although for both MDMs *E*_{binding} decreases with increasing number of H₂ molecules, the decrease in *E*_{binding} is more significant in the case of Sc. Furthermore, its binding energies for all *n* are well within

the range (20–40 kJ/mol H₂) resulting in H₂ storage at ambient temperature.

Typically H₂ binds to TMs through charge Kubas interactions. Such electrostatic interactions are consistent with small changes in the H–H bond length, which is true for our systems as well as seen from Table 1. (Our calculated value for the H–H bond distance in the free molecule is 0.750 Å.) This decrease in H–H distances with *n* can be attributed to electron donation from hydrogen sigma bonding orbital to d orbital of metal, but as the number of H₂ molecules increases, electron donation from sigma bonding orbital of each H₂ to d orbitals of metal reduces due to competition of more H₂ molecules. Consequently the H₂ bond length starts approaching its equilibrium value when significant numbers of H₂ molecules interact with MOF-5:M₂.

Lately many studies are focused on Boron-substituted metal-decorated MOFs.^{44,45} Their results prove that B substitution increases the interaction energy of these metals with MOFs and carbon-based nanomaterials. We have also studied 1,4 boron substituted Sc- and Ti-decorated MOF-5 and found in agreement with these results that boron substitution of MOF-5 increases its interaction energy by almost 100% with Sc and Ti (to −484.9 and −502.75 kJ/mol, respectively). To investigate whether boron substitution can further avoid the TM clustering problem in our systems, to start with, three Sc and Ti atoms were decorated on 1,4-boron-substituted MDMs on each side of benzene ring at low M–M distance of 1.511 Å. As in the case of MOF-5:Sc₆, upon relaxation, Sc atoms were found to be significantly apart (3.1 Å) with a Bader charge of

**Figure 5.** Relaxed structures of (a) MOF:2B:Sc₂ and MOF:2B:Sc₂:2*n*H₂ (b) 2H₂, (c) 4H₂, (d) 6H₂, (e) 8H₂, and (f) 10H₂.

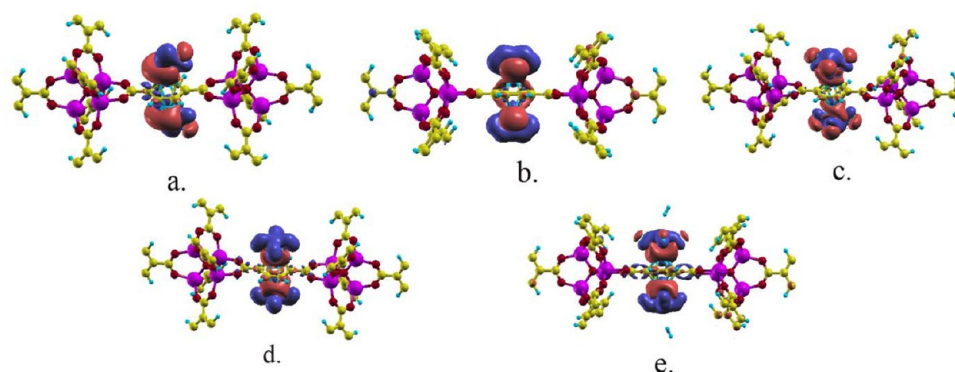


Figure 6. Difference charge density plots of MOF:Sc:2*n*H₂ (a) 2H₂, (b) 4H₂, (c) 6H₂, (d) 8H₂, (e) 10H₂.

1.13 e/Sc. Interestingly the Ti–Ti distances and charge increased to 2.42 Å and 0.71 e/Ti in 1,4-B substituted MOF-5 compared with MOF-5:Ti₆, but these are still not large enough to avoid clustering completely (Figure S6 of the Supporting Information).

As Sc atoms continue to not cluster even in presence of B atoms, we have further studied adsorption of up to 5H₂ molecules per metal. (See Figure 5.) The calculated E_{binding} values, presented in Table 2, are decreased slightly by B substitution. The only noticeable difference is in the orientation of H₂ molecule: parallel in B-substituted Sc-decorated MOF-5 and perpendicular in non-B-substituted Sc-decorated MOFs.

The above discussions suggest Sc to be a potential dopant for MOF-5 in the view of H₂ storage. Charge density calculations have been done to investigate the charge distribution over the entire systems for all MOF:Sc:2*n*H₂ structures (*n* = 1–5). DCD plots show the charge transfer; blue reign indicates the charge loss, whereas red reign indicates charge gain. Electron transfer from hydrogen to metals can be clearly identified from DCC plots of these systems (Figure 6).

To estimate the storage capacity in the systems under investigation, we assume that all metal sites are saturated, that is, 5H₂ are adsorbed around every metal atom, and that no other sites are populated. Because each formula unit (f.u.) contains six metal atoms, Zn₄O(BDC)₃M₆, this corresponds to a total adsorption of 30 H₂ molecules equivalent to a hydrogen uptake of 5.81, 5.72, and 5.86 wt % for Sc-decorated MOF-5, Ti-decorated MOF-5, and Sc-decorated 1,4-boron-substituted MOF-5, respectively. Therefore, Sc-decorated MOF-5s with their avoidance of metal clustering, suitable H₂ binding energies, and high gravimetric H₂ storage capacities are excellent candidates for achievement of practical applications of H₂ storage under ambient conditions.

Therefore, we have analyzed light TM decoration of MOF-5 and its subsequent effect on its hydrogen storage properties. Our results suggest that in these systems Ti suffers from clustering but Sc avoids this problem. The calculated binding energies are found to be in the desired range for hydrogen storage at room temperature. Boron substitution increases the interaction energy. Both Sc- and Ti-decorated MOF-5 adsorb 5H₂ per metal atom, with gravimetric storage of 5.81 and 5.72 wt %, respectively. Because of high storage and desired binding affinity, Sc-decorated MOF-5 is found to be an excellent hydrogen storage candidate for room-temperature applications.

■ COMPUTATIONAL METHODOLOGY

All calculations have been performed using the Vienna ab initio simulations package (VASP)^{46,47} with DFT planewave-pseudopotential-based approach. We have used the projector-augmented wave (PAW)^{48,49} approach to evaluate all the properties. The PAW potentials with the valence states 3p4s3d for Sc, d3s1 for Ti 2s2p for C, 2s2p for O, d10p2 for Zn, 1s for H, and s2p1 for B were used. A kinetic energy cutoff of 520 eV was employed for primitive cell calculations, whereas 400 eV cutoff was taken for full-unit cell calculations. For Sc-*n*H₂ systems, 330 eV cutoff was taken with spin-polarized calculations. All geometry optimizations were carried out without any geometry constraint. All forces were calculated using the Hellmann–Feynman theorem. Geometries were considered optimized with maximum force found smaller than 0.01 eV/Å. Real-space projections were used to evaluate PAW character of wave functions. The primitive cell of MOF-5 was built from the crystal structure of MOF-5 that was taken from experimental data,⁵⁰ and a 2 × 2 × 2 k-point grid generated by Monkhorst Pack scheme⁵¹ was applied to it. For obtaining the atomic charges, Bader analysis⁴⁴ was performed. Molecular DFT calculation of SC₂–BDC were performed at the B3LYP^{52,53}/6-311+g(d) level using Gaussian09 program package.⁵⁴ Solvent effects were introduced using the polarizable continuum solvation model (PCM).⁵⁵

■ ASSOCIATED CONTENT

● Supporting Information

Discussion of structural features of M-*n*H₂ systems, optimized geometries of M-*n*H₂ and MOF-5:Ti₂:*n*H₂ systems, geometries of MOF-5:2B:M₆ before and after relaxation, plot of Bader charges, and optimized geometries of SC₂–BDC systems. This material is available free of charge via Internet at <http://pubs.acs.org>.

■ AUTHOR INFORMATION

Corresponding Author

*E-mail: s.pal@ncl.res.in. Phone: +91 20 25902600. Fax: +91 20 25902601.

Notes

The authors declare no competing financial interest.

■ ACKNOWLEDGMENTS

We acknowledge the computational facilities of the Center of Excellence in Scientific Computing at National Chemical Laboratory, Pune. We also thank the FP7- NMP-EU-India-2

collaborative project HYPOMAP on “New materials for hydrogen-powered mobile applications” for providing financial support. M.D. thanks UGC, India for grant of Senior Research Fellowship. T.A.M. would like to acknowledge FUTURA for her postdoctoral scholarship. R.A. would like to thank FORMAS for funding. S.P. acknowledges the J. C. Bose Fellowship grant of DST, India and Shanti Swarup Bhatnagar fellowship grant of CSIR, India toward completion of this work.

REFERENCES

- (1) Schlappbach, L.; Zuttel, A. *Nature* **2001**, *414*, 353–353.
- (2) Kelkar, T.; Pal, S.; Kanhere, D. G. *ChemPhysChem* **2008**, *9*, 928–934.
- (3) Kumar, R. M.; Subramanian, V. *Int. J. Hydrogen Energy* **2011**, *36*, 10737–10747.
- (4) Eddaoudi, M.; Li, H.; Reineke, T.; Fehr, M.; Kelley, D.; Groy, T. L.; Yaghi, O. M. *Top. Catal.* **1999**, *9*, 105–111.
- (5) Rowsell, J. L. C.; Yaghi, O. M. *J. Am. Chem. Soc.* **2006**, *128*, 1304–1315.
- (6) Bordiga, S.; Vitillo, J. G.; Ricchiardi, G.; Regli, L.; Cocina, D.; Zecchina, A.; Bjørnar, A.; Morten, B.; Jasmina, H.; Lillerud, K. P. *J. Phys. Chem. B* **2009**, *109*, 18237–18242.
- (7) Kaye, S. S.; Long, J. R. *J. Am. Chem. Soc.* **2005**, *127*, 6506–6507.
- (8) Lochan, R. C.; Head-Gordon, M. *Phys. Chem. Chem. Phys.* **2006**, *8*, 1357–1370.
- (9) Niu, J.; Rao, B. K.; Jena, P. *Phys. Rev. Lett.* **1992**, *68*, 2277–2280.
- (10) Rao, B. K.; Jena, P. *Europhys. Lett.* **1992**, *20*, 307–312.
- (11) Niu, J.; Rao, B. K.; Khanna, S. N.; Jena, P. *Chem. Phys. Lett.* **1991**, *230*, 299–305.
- (12) Maseras, F.; Lledos, A.; Clot, E.; Eisenstein, O. *Chem. Rev.* **2000**, *100*, 601–636.
- (13) Gagliardi, L.; Pyykko, P. *J. Am. Chem. Soc.* **2004**, *126*, 15014–15015.
- (14) Maark, T. A.; Pal, S. *Int. J. Hydrogen Energy* **2010**, *35*, 12846–12857.
- (15) Chandrakumar, K. R. S.; Ghosh, S. K. *Chem. Phys. Lett.* **2007**, *447*, 208–214.
- (16) Kiran, B.; Kandalam, A. K.; Jena, P. *J. Chem. Phys.* **2006**, *124*, 224703.
- (17) Durgun, E.; Jang, Y.-R.; Ciraci, S. *Phys. Rev. B* **2007**, *76*, 073413.
- (18) Zhao, Y.; Kim, Y. H.; Dillon, A. C.; Heben, M. J.; Zhang, S. B. *Phys. Rev. Lett.* **2005**, *94*, 155504.
- (19) Phillips, A. B.; Shivaram, B. S. *Phys. Rev. Lett.* **2008**, *100*, 105505.
- (20) Yildirim, T.; Ciraci, S. *Phys. Rev. Lett.* **2005**, *94*, 175501.
- (21) Zhou, W.; Yildirim, T.; Durgun, E.; Ciraci, S. *Phys. Rev. B* **2007**, *76*, 085434.
- (22) Suttisawat, Y.; Rangsunvigit, P.; Kitiyanan, B.; Williams, M.; Ndungu, P.; Lototsky, M.; Nechaev, A.; Linkov, V.; Kulprathipanja, S. *Int. J. Hydrogen Energy* **2009**, *34*, 6669–6675.
- (23) Kim, B. J.; Lee, Y. S.; Park, S. J. *Int. J. Hydrogen Energy* **2008**, *33*, 4112–4115.
- (24) Zubizarreta, L.; Menendez, J.; Pis, J.; Arenillas, A. *Int. J. Hydrogen Energy* **2009**, *34*, 3070–3076.
- (25) Lee, H.; Choi, W. I.; Ihm, J. *Phys. Rev. Lett.* **2006**, *97*, 056104.
- (26) Patchkovskii, S.; Tse, J. S.; Yurchenko, S. N.; Zhechkov, L.; Heine, T.; Seifert, G. *Proc. Natl. Acad. Sci. U.S.A.* **2005**, *102*, 10439–10444.
- (27) Heine, T.; Zhechkov, L.; Seifert, G. *Phys. Chem. Chem. Phys.* **2004**, *6*, 980–984.
- (28) Sun, Q.; Jena, P.; Wang, Q.; Marquez, M. *J. Am. Chem. Soc.* **2006**, *128*, 9741–9745.
- (29) Chandrakumar, K. R. S.; Ghosh, S. K. *Nano Lett.* **2007**, *8*, 13–9.
- (30) Forst, C. J.; Slycke, J.; Van Vliet, K. J.; Yip, S. *Phys. Rev. Lett.* **2006**, *96*, 175501.
- (31) Kim, Y. H.; Zhao, Y.; Williamson, A.; Heben, M. J.; Zhang, S. B. *Phys. Rev. Lett.* **2006**, *96*, 016102.
- (32) Chen, P.; Wu, X.; Lin, J.; Tan, K. L. *Science* **1999**, *285*, 91–93.
- (33) Blomqvist, A.; Arajo, C. M.; Srepusharawoot, P.; Ahuja, R. *Proc. Natl. Acad. Sci. U.S.A.* **2007**, *104*, 20173–20176.
- (34) Han, S. S.; Goddard, W. A. *J. Am. Chem. Soc.* **2007**, *129*, 8422–8423.
- (35) Venkataraman, N.; Sahara, R.; Mizuseki, H.; Kawazoe, Y. *Int. J. Mol. Sci.* **2009**, *10*, 1601–1608.
- (36) Sun, Y. Y.; Lee, K.; Kim, Y. H.; Zhang, S. B. *Appl. Phys. Lett.* **2009**, *95*, 033109.
- (37) Zou, X.; Cha, M. H.; Kim, S.; Nguyen, M. C.; Zhou, G.; Duan, W.; Ihm, J. *Int. J. Hydrogen Energy* **2010**, *35*, 198–203.
- (38) Han, S. S.; Mendoza-Cortés, J. L.; Goddard, W. A., III. *Chem. Soc. Rev.* **2009**, *38*, 1460–1476.
- (39) Srinivasu, K.; Ghosh, S. K. *J. Phys. Chem. C* **2011**, *115*, 16984–16991.
- (40) Han, S. S.; Goddard, W. A. *J. Phys. Chem. C* **2008**, *112*, 13431–12436.
- (41) Sun, Q.; Wang, Q.; Jena, P.; Kawazoe, Y. *J. Am. Chem. Soc.* **2005**, *127*, 14582–14583.
- (42) Krasnov, P. O.; Ding, F.; Singh, A. K.; Yakobson, B. *J. Phys. Chem. C* **2007**, *111*, 17977–17980.
- (43) Dixit, M.; Maark, T. A.; Pal, S. *Int. J. Hydrogen Energy* **2011**, *36*, 10816–10827.
- (44) Henkelman, G.; Arnaldsson, A.; Jonsson, H. *Comput. Mater. Sci.* **2006**, *36*, 354–360.
- (45) Kubo, M.; Shimojima, A.; Okubo, T. *J. Phys. Chem. C* **2012**, *116*, 10260–10265.
- (46) Kresse, G.; Furthmüller, J. *Comput. Mater. Sci.* **1996**, *6*, 15–50.
- (47) Kresse, G.; Furthmüller, J. *Phys. Rev. B* **1996**, *54*, 11169–11186.
- (48) Kresse, G.; Joubert, D. *Phys. Rev. B* **1999**, *59*, 1758–1775.
- (49) Blochl, P. E. *Phys. Rev. B* **1994**, *50*, 17953–17979.
- (50) Li, H.; Eddaoudi, M.; O’Keeffe, M.; Yaghi, O. M. *Nature* **1999**, *402*, 276–279.
- (51) Monkhorst, H. J.; Pack, J. D. *Phys. Rev. B* **1976**, *13*, 5188–5192.
- (52) Becke, A. D. *J. Chem. Phys.* **1993**, *98*, 5648–52.
- (53) Stephens, P. J.; Devlin, F. J.; Chabalowski, C. F.; Frisch, M. J. *J. Phys. Chem.* **1994**, *98*, 11623–11627.
- (54) Trucks, G. W.; Schlegel, H. B.; Scuseria, G. E.; Robb, M. A.; Cheeseman, J. R.; Scalmani, G.; Barone, V.; Mennucci, B.; Petersson, G. A. et al. *Gaussian 09*, revision A.1; Gaussian, Inc.: Wallingford, CT, 2009.
- (55) Cossi, M.; Scalmani, G.; Rega, N.; Barone, V. *J. Chem. Phys.* **2002**, *117*, 43–54.